Struct Chem (2013) 24:559–571
DOI 10.1007/s11224-012-0108-x

ORIGINAL RESEARCH

A DFT study of hydrogen bond interactions between oxidative 2′-deoxyadenosine nucleotides and RNA nucleotides

Jie Shen · Haijun Wang · Yongmei Xia

Received: 15 March 2012 / Accepted: 25 July 2012 / Published online: 14 August 2012

Abstract In this study, the interactions between oxidative 2′-deoxyadenosine nucleotides (2OHA, 8OHA, 8OXOA, fapyA) and canonical ribonucleotides (A, C, G, U) were investigated at B3LYP level with 6-31G(d) basis set. The binding energies calculated were corrected for the basis set superposition error at the same level. The result shows that syn 8OXOA:G complex is the most stable among all the complexes. According to energetic analysis, the species and position of substitution of 2′-deoxyadenosine nucleotide significantly influence the stability of conformers. The intermolecular and intramolecular hydrogen bonds (HBs) were characterized based on atoms in molecules theory (AIM) and natural bond orbital (NBO) analysis, indicating that the type and geometry of HB significantly influence the stability of monomer and complex. Furthermore, in most cases, the intramolecular HBs in monomer and complex exhibit similar properties because they own nearly the same geometry and parameters obtained from AIM and NBO analysis.

Keywords DFT study · Hydrogen bond · Oxidative 2′-deoxyadenosine nucleotides · RNA nucleotides

Introduction

There are enormous researches on the intermolecular or intramolecular hydrogen bond (HB) interactions of nucleosides [1–6] and nucleotides [7, 8]. Shishkin et al. [9] investigated the structure and relative stability of 2′-deoxyribonucleotides at B3LYP/6-31G(d,p). Non-Watson–Crick base pair resulted from noncanonical nucleobases has gained great interest because of the CH···O/N interaction [10–13] and their biological function [14, 15]. Qiu et al. [16] reported that the oxidative guanine can form more stable complex with cytosine. Popelier and Xue et al. [17] investigated the interactions of 37 base pairs between 8-position-substituted G and unmodified C, it is observed that the presence of an electron-withdrawing group on the 8-position of G forms a more stable base pair with C. This conclusion is in good agreement with the study [18] that 8-CH_3O–G:C has the greater energy than 8-NO_2–G:C. In the case of CH···O in non-Watson–Crick base pair, Guerra et al. [19] argued that the distance between the C–H and O is too far to be considered as a hydrogen–bonding interaction. Maybe the present method and criterion adapt to conventional HB are improper to C–H···O. This supplies an opportunity for theoretical methods to obtain reliable information and characterize intramolecular C–H···O bonds.

Besides intermolecular HB, intramolecular HB is also responsible for stability and function of nucleotides. A research of molecular structure of canonical 2′-deoxyribonucleotides [20] demonstrated that the intramolecular OH···O and CH···O bonds may significantly influence the equilibrium conformation and relative stability of conformers. Another investigation [3, 21] showed that intramolecular NH···O and CH···O bonds between base and phosphate group are responsible for stabilization of conformation with respect to ribose, rotation around glycosidic bond. It should be noted that

---

Electronic supplementary material The online version of this article (doi:10.1007/s11224-012-0108-x) contains supplementary material, which is available to authorized users.

J. Shen · Y. Xia (✉)
State Key Laboratory of Food Science and Technology,
Jiangnan University, Wuxi 214122, China
e-mail: ymxia@jiangnan.edu.cn

J. Shen · H. Wang · Y. Xia
School of Chemical and Material Engineering,
Jiangnan University, Wuxi 214122, China

although CH···O is common in isolated nucleobase, it still ambiguous to define this kind of interaction as no comparison with model compounds was provided.

To the date, study on the intermolecular HB interaction has been focused on DNA nucleobases. Moreover the investigations of intramolecular HB interaction merely focus on mononucleotides or mononucleosides. To further understand the overall interaction of nucleotides there is a need to study the complete nucleotide consisting of sugar–phosphate-base including RNA. In this article, we investigate the interaction of anti/syn conformers [22, 23] of four oxidative 2′-deoxyadenosine nucleotides (2OHA, 8OHA, 8OXOA, fapyA) [24–27] caused by UV light, ionizing radiation and other chemical mutagen [28] and RNA nucleotides (A, C, G, U). Furthermore, the intramolecular HB interaction in monomers and complexes are also taken into account. This study will provide a prediction of interaction between oxidative nucleotides of DNA and RNA nucleotides.

Computational details

Geometry optimizations were performed in the gas phase using B3LYP, which is the density functional theory with the Becke's three-parameter exchange functional and the gradient-corrected functional of Lee et al. [29–31] to accurately describe the conformers the standard 6-31G(d) basis set was employed in conjunction with the B3LYP method. This function with basis set was applied not only in nucleobases but also in nucleosides and nucleotides [32–34]. It has been proven that this level of theory provides accurate geometries for hydrogen-bonded complexes involving the natural nucleobase [35]. Calculations of vibrational frequencies were also carried out to confirm the optimized structures are in their minima. The binding energy was evaluated as the difference between the total energy of a complex and the energies of its' monomers [36]. In this article, the binding energy including zero-point vibrational energy (ZPVE) correction of every complex was obtained at B3LYP/6-31G(d). And this binding energy (ΔE^{ZPVE}) of the complex was corrected for the basis set superposition error (BSSE) [37] by the Boys-Bernardi counterpoise method [38]. In addition, the binding energy of the complex was also calculated using B3LYP method with aug-cc-pVDZ, 6-311++G(d,p), 6-311++G(d), 6-31G(d), respectively. And these binding energies (ΔE) which were obtained by single point calculations of complex and monomers contained counterpoise correction to account for the BSSE. All the calculations were carried out with GAUSSIAN 03 program [39].

In this study, the atoms in molecules (AIM) analysis [40] was employed as one of the most powerful approaches to characterize the HBs both in complexes and monomers. The "AIM" theory successfully demonstrates chemical bonds based on the topological properties of the electronic charge density. According to this theory, the existence of HB is established based on the presence of a bond critical point (BCP) and a bond path between hydrogen donor and acceptor. To identify the HB, we employed the criteria proposed by Popelier [41–43] that the value of electron density (ρ_c) at the BCP was set at 0.002–0.040 a.u. and the value of Laplacian ($\bigtriangledown^2\rho_c$) was set at 0.02–0.15 a.u. In order to obtain the valuable information about the influence of HB interaction on electrons around the critical point, the local kinetic energy density, $G(r)$ and the local electron potential energy density, $V(r)$ were taken into account [44]. The evaluation of $G(r)$ was proposed by Abramov [45] according to the following equation:

$$G(r) = \left(\frac{3}{10}\right)\left(3\pi^2\right)^{2/3}\rho_c^{3/5} + \left(\frac{1}{6}\right)\nabla^2\rho_c \tag{1}$$

Furthermore, $G(r)$ is related to $V(r)$ through the local statement of the virial theorem [40, 46]:

$$V(r) = (\mathrm{h}^2/4\mathrm{m})\nabla^2\rho_c - 2G(r) \tag{2}$$

The HB energy (E_{HB}) suggested by Espinosa et al. [44, 1998] is estimated in terms of $V(r)$:

$$E_{\mathrm{HB}} = \frac{1}{2}V(r) \tag{3}$$

This relationship named as EML equation describes a proportionality between HB energy and local electron potential energy density, offering the possibility to directly calculate the HB energy based on Bader's theory. The AIM analysis was performed using AIM2000 program.

Natural bond orbital (NBO) analysis [47–49] was carried out at B3LYP/6-31G(d) level. This analysis provides the information including charge transfer process and hyperconjugative interaction. The estimation of hyperconjugative interaction from the second order perturbation energy can be expressed as

$$E^{(2)} = \Delta E_{\mathrm{ij}} = qi\left[F^2_{(\mathrm{i,j})}/\left(E_{\mathrm{i}} - E_{\mathrm{j}}\right)\right] \tag{4}$$

where qi denotes the donor orbital occupancy, $F_{(\mathrm{i,j})}$ is the off-diagonal NBO Fock matrix element, and E_{i}, E_{j} are the diagonal element.

Result and discussion

Binding energy analysis

The values of ΔE^{ZPVE} calculated at B3LYP/6-31G(d) level are summarized in Table 1. The values of ΔE evaluated at B3LYP method, respectively in combination with aug-cc-pVDZ, 6-311++G(d,p), 6-311++G(d), 6-31G(d) are shown in Tables 2, 3, 4, and 5. It is obvious that for every oxidative 2′-deoxyadenosine nucleotide, the orders of binding energies of it and the four RNA nucleotides from the strongest to the weakest are the same at all the applied computational levels. Furthermore, the values of ΔE calculated at different basis set are similar. It is worth noting that combined with B3LYP method, the above basis sets no matter the larger or smaller ones are in good agreement to calculate such neutral complex of nucleotides. Thus, the complexes in this study are proper to be evaluated employing those basis sets. It is revealed that the values of ΔE of s8OHA:A and s8OHA:C complexes are much larger than other complexes. This phenomenon is due to hydrogen migration which will be discussed subsequently. Moreover, the values of ΔE obtained from 6–31G(d) basis set are the most negative while the ones attained from aug-cc-pVDZ basis set are the least negative. This is similar to the study that 6-311++G(d,p) leads to lower calculated energies than aug-cc-pVDZ [50]. The ΔE^{ZPVE} and ΔE obtained from B3LYP/6-31G(d) level were compared. In most cases, the ZPVE corrections range between 1 and 3 kcal/mol indicating that ZPVE correction has effect on the binding energy. However, it has no influence on the orders of binding energies of the complexes at all.

It is known that natural nucleotides exist in the form of anti conformation. Meanwhile, it is suggested that there occurs the syn conformer of modified nucleotide [23, 51]. As it can be seen in Table 1, it is obvious that the RNA nucleotides are more preferable to pair to syn 8OXOA (s8OXOA) than anti 8OXOA (8OXOA) as far as the values of binding energies are concerned. This result is consistent with the investigation [52] that 8-oxopurines including 8-oxo-adenine can cause a flip in nucleoside conformation from anti to syn, leading to mispairing and mutagenesis [53]. Furthermore, Taniguchi and Kool [54] found that natural oxopurines adopt the syn orientation and change pairing preferences because of their altered shapes. Here, the binding energies may shed light on the syn preference of s8OXOA and 8-oxopurines. In addition, as well as 8OXOA, 8OHA is in favor of syn conformation to combine with RNA nucleotides. However, as for 2OHA and fapyA, there is no explicit conclusion on which orientation significantly influences the pairing according to energetic analysis. On the other hand, the anti and syn orientation of every oxidative 2′-deoxyadenosine nucleotide form the most stable complexes with different RNA nucleotides. This is similar to the study of 8-OXO-2′-deoxyguanosine [55, 56] showing that it is, respectively in anti and syn conformation to pair to dC and dA. Hamm et al. [57] argued that the glycosidic bond conformation of 8-OXO-2′-deoxyguanosine depends on the opposite base. Moreover, there has been a discussion [58–60] on whether syn-anti conformer significantly influences DNA replication selectivity. In addition, this selectivity in the absence of enzymes relies on complementary HB and pair geometry

Table 1 Binding energies including ZPVE ΔE^{ZPVE} (kcal/mol) of complexes calculated at B3LYP/6-31G(d) level

Pair	ΔE^{ZPVE}
8OXOA:A	−3.96
8OXOA:C	−4.28
8OXOA:G	−12.86
8OXOA:U	−11.56
s8OXOA:A	−8.95
s8OXOA:C	−13.80
s8OXOA:G	−20.24
s8OXOA:U	−14.29
8OHA:A	−4.48
8OHA:C	−5.05
8OHA:G	−12.98
8OHA:U	−11.67
s8OHA:A	−14.45
s8OHA:C	−20.19
s8OHA:G	−14.07
s8OHA:U	−17.24
2OHA:A	−10.00
2OHA:C	−10.20
2OHA:G	−12.01
2OHA:U	−13.97
s2OHA:A	−5.20
s2OHA:C	−6.59
s2OHA:G	−12.25
s2OHA:U	−12.01
fapyA:A	−4.52
fapyA:C	−5.24
fapyA:G	−10.88
fapyA:U	−9.83
sfapyA:A	−5.90
sfapyA:C	−8.29
sfapyA:G	−5.27
sfapyA:U	−6.15

Table 2 Binding energies ΔE (kcal/mol) of complexes including 8OXOA calculated at B3LYP with various basis sets

Pair	ΔE (kcal/mol)			
	aug-cc-pvdz	6-311++G**	6-311++G*	6-31G*
8OXOA:A	−4.56	−4.72	−4.57	−4.95
8OXOA:C	−4.87	−5.18	−5.01	−5.40
8OXOA:G	−15.29	−15.33	−15.12	−15.73
8OXOA:U	−13.81	−13.81	−13.54	−13.99
s8OXOA:A	−10.97	−11.44	−11.41	−12.19
s8OXOA:C	−23.82	−24.25	−24.27	−25.13
s8OXOA:G	−25.27	−25.18	−25.05	−25.55
s8OXOA:U	−17.22	−17.22	−17.06	−17.60

Table 3 Binding energies ΔE (kcal/mol) of complexes including 8OHA calculated at B3LYP with various basis sets

Pair	ΔE (kcal/mol)			
	aug-cc-pvdz	6-311++G**	6-311++G*	6-31G*
8OHA:A	−5.38	−5.49	−5.36	−5.75
8OHA:C	−6.02	−6.30	−6.14	−6.52
8OHA:G	−15.32	−15.36	−15.18	−15.89
8OHA:U	−13.60	−13.87	−13.65	−14.06
s8OHA:A	−78.93	−79.11	−77.24	−77.58
s8OHA:C	−230.71	−241.44	−228.25	−229.75
s8OHA:G	−17.36	−17.85	−17.86	−19.20
s8OHA:U	−20.20	−20.58	−20.14	−20.88

Table 4 Binding energies ΔE (kcal/mol) of complexes including 2OHA calculated at B3LYP with various basis sets

Pair	ΔE (kcal/mol)			
	aug-cc-pvdz	6-311++G**	6-311++G*	6-31G*
2OHA:A	−12.82	−13.06	−12.69	−13.44
2OHA:C	−12.91	−13.18	−12.89	−14.07
2OHA:G	−14.91	−15.33	−15.28	−16.44
2OHA:U	−16.83	−17.13	−16.69	−17.71
s2OHA:A	−6.19	−6.37	−6.25	−6.77
s2OHA:C	−9.29	−9.83	−9.70	−9.94
s2OHA:G	−15.30	−15.53	−15.32	−15.95
s2OHA:U	−14.52	−14.80	−14.55	−14.92

Table 5 Binding energies ΔE (kcal/mol) of complexes including fapyA calculated at B3LYP with various basis sets

Pair	ΔE (kcal/mol)			
	aug-cc-pvdz	6-311++G**	6-311++G*	6-31G*
fapyA:A	−5.24	−5.49	−5.35	−5.74
fapyA:C	−6.81	−6.45	−6.29	−6.63
fapyA:G	−13.11	−13.38	−13.20	−13.82
fapyA:U	−11.88	−12.17	−11.90	−12.27
sfapyA:A	−7.39	−7.25	−7.17	−7.53
sfapyA:C	−10.23	−10.29	−10.21	−10.28
sfapyA:G	−10.93	−11.01	−11.00	−11.13
sfapyA:U	−9.15	−8.93	−8.88	−8.89

[54] which can be considered as the important factors to determine translation from oxidative DNA to RNA.

It is revealed that the binding energies of complexes including anti 8OHA are smaller than that of complexes containing anti 8OXOA. In most cases syn 8OHA has stronger binding ability than syn 8OXOA. In brief, it can be shown that A with hydroxyl substituted at 8-position is more favorable to combine with nucleotides than that with carbonyl substituted at the same position both in anti and syn forms. In addition, the complexes with anti/syn 8OXOA are more stable than that with anti/syn fapyA. In the case of OH, respectively substituted at 2 and 8 position of A, they have different binding ability with RNA nucleotides. To sum up, it is obvious that the species and position of substitution of A have a significant effect on the stability of complex. It was proposed that the substituent effects on noncovalent interactions result from alterations of the intermolecular HB distances and the binding energy of the pair [61, 62] and it should be underlined that the binding interaction of complexes is determined by intermolecular HB to a great extent which will be explained subsequently.

Geometry and property of intermolecular HB

Tables 6, 7, 8, and 9 show the intermolecular HBs between oxidative $2'$-deoxyadenosine and RNA nucleotides. In most situation, the electron density (ρ_c) and Laplacian of electron density ($\nabla^2\rho_c$) of NH···N/O and OH···O/N are, respectively within 0.03–0.04 and 0.07–0.12 a.u., showing that these HBs belong to strong ones and result in significant stabilization of complexes. This agrees well with a previous study [10] revealing that these HBs play a dominate role in the base pair stability. The ρ_c and$\nabla^2\rho_c$ value of CH···N are about 0.01 and 0.03 a.u., leading to a weaker interaction. These results above are in good agreement with NBO analysis that the values of $E^{(2)}$ of NH···N/O and OH···O/N are much higher than those of CH···N. The CH···Os have ρ_c of 0.004 a.u. and $\nabla^2\rho_c$ of 0.018 a.u., indicating that these parameters approach the lower limit of criteria of HB. Therefore, the definition of CH···O always exists controversial. Some studies [10, 63] considered the formation of CH···O as a weak H-bond, while others [11, 64] view this formation as electronic interaction rather than H-bonding interaction. One of the reasons in favor of the latter is that the donor–acceptor orbital interaction corresponding with this HB cannot be found [19]. However, for the intermolecular CH···O investigated here, the values of $E^{(2)}$ which are smaller than 0.6 kcal/mol provide the information considered as a useful method for charactering HB that there occurs a very weak donor–accepter orbital interaction between O lone pair orbital and C–H σ^* antibonding orbital. Thus, the intermolecular CH···O in the complexes above should be classified as real but rather weak HB.

Since theoretical studies are able to obtain a complete description of both topological and energetic properties at critical points, many researches focus on the correlations between parameters such as $G(r)$ and HB distance [44, 65],

Table 6 Bond length (d), angle (θ), density (ρ_c), Laplacian of electron density ($\nabla^2\rho_c$), the local kinetic energy density ($G(r)$), local electron potential energy density ($V(r)$), HB energy (E_{HB}), and second order perturbation energy ($E^{(2)}$)for complexes including 8OHA Calculated at B3LYP/6-31G(d) level

Pair	H-bond	d (Å)	θ (°)	ρ_c (a.u.)	$\nabla^2\rho_c$ (a.u.)	$G(r)$ (a.u.)	$V(r)$ (a.u.)	E_{HB} (kcal/mol)	$E^{(2)}$ (kcal/mol)
Anti									
8OHA:A	N10–H···N1	2.035	175.3	0.026	0.070	0.018	−0.019	−5.98	22.15
	C2–H···N1	2.514	147.1	0.011	0.031	0.007	−0.006	−1.83	5.17
8OHA:C	N8–H···N1	2.009	175.2	0.028	0.073	0.020	−0.021	−6.49	15.53
	C2–H···N3	2.471	143.9	0.012	0.035	0.008	−0.006	−2.01	2.89
8OHA:G	N10–H···O11	1.871	177.5	0.032	0.096	0.025	−0.026	−8.25	30.53
	N1–H···N1	1.909	177.9	0.035	0.090	0.026	−0.029	−9.12	36.06
8OHA:U	N10–H···O8	1.924	173.8	0.028	0.085	0.022	−0.022	−6.87	15.37
	N3–H···N1	1.855	178.0	0.039	0.099	0.029	−0.034	−10.62	29.48
	C2–H···O7	2.890	131.4	0.004	0.016	0.003	−0.002	−0.60	0.52
Syn									
s8OHA:A	N10–H···N7	1.725	170.3	0.051	0.124	0.041	−0.051	−15.91	78.31
	O8–H···N1	1.461	173.9	0.085	0.189	0.078	−0.109	−34.29	87.02
s8OHA:C	N7–H···N8	1.823	169.5	0.041	0.107	0.032	−0.037	−11.61	50.94
	N3–H···O8	1.853	177.5	0.033	0.099	0.026	−0.027	−8.63	34.72
s8OHA:G	N10–H···O11	1.970	169.7	0.025	0.077	0.019	−0.019	−5.93	13.14
	N1–H···N7	1.842	166.4	0.039	0.105	0.031	−0.035	−10.98	27.33
	O8–H···N10	1.865	163.7	0.038	0.095	0.028	−0.033	−10.30	23.28
s8OHA:U	N10–H···O8	1.989	169.7	0.024	0.074	0.018	−0.018	−5.50	19.24
	N3–H···N7	1.794	173.3	0.043	0.113	0.034	−0.040	−12.62	68.63
	O8–H···O7	1.736	175.9	0.041	0.129	0.036	−0.039	−12.16	56.35

$V(r)$ and $G(r)$ [66], ρ_c and $G(r)$ [67]. Wojtulewski and Grabowski [68] demonstrated the linear correlation between $G(r)$ and E_{HB} at the critical point of H···O bond. The similar result concerning the relationship between $G(r)$ and E_{HB} was also observed in this study that there exist the excellent linear correlations between $G(r)$ and E_{HB} for the intermolecular NH···N/O and OH···N with the correlation coefficient amounting to 0.996 and 0.999, respectively (Figs. 1, 2). Thus, it provides the approach to obtain the accessible $V(r)$ or E_{HB} directly from Abramov relation which may be successfully used for HBs. In addition, it is indicated that the theoretical electron density may be useful to check the Abramov approach [68]. Furthermore, as in Fig. 3, the decreased $G(r)$ of every intermolecular HB mentioned above is related exponentially with the increased corresponding HB distance. According to the exponential fittings of $G(r)$ versus HB distance of NH···N/O and OH···N, the correlation coefficients are, respectively 0.994, 0.992, and 0.999, indicating the good negative correlation between the local kinetic energy density and HB geometry. It can be explained that a lower accumulation of electrons implies less repulsion at critical point [44].

As it can be seen in Tables 6, 7, 8, and 9, two energetic parameters, E_{HB} and $E^{(2)}$ representing different physical meaning were employed to estimate the strength of HB. For E_{HB}, it denotes the binding energy of HB based AIM analysis implying that the more negative E_{HB} is corresponding to the stronger HB interaction. On the other hand, $E^{(2)}$ generated by NBO analysis is applied to evaluate the charge transfer from proton acceptor to σ^* antibonding orbital of proton donor. Thus, the increasing $E^{(2)}$ reflects the strengthing HB. In this study, it was found that the values of E_{HB} and $E^{(2)}$ of intermolecular NH···N from the strongest to the weakest were −5.98, 22.15, and −3.73, 11.11 kcal/mol. In the case of NH···O, the maximum value of $E^{(2)}$ is 51.02 kcal/mol with the corresponding E_{HB} of −14.41 kcal/mol, at the same time, the minimum value of $E^{(2)}$ of 0.86 kcal/mol is associated with the value of E_{HB} of −0.53 kcal/mol. Meanwhile, the values of E_{HB} of intermolecular OH···N are within the range −34.29–−5.95 kcal/mol, the corresponding values of $E^{(2)}$ are from 87.02 to 0.11 kcal/mol. In a word, all the results above show that E_{HB} is in good agreement with $E^{(2)}$ in evaluating the strength of intermolecular HB of nucleotides.

In addition, the geometry of the complexes, especially the H-bond distance and angle, also supply another indication of the interaction [69]. It is found that the distance of NH···N/O and OH···O/N are between 1.7 and 2.0 Å, and their angle vary from 166° to 177°, the length and angle of OH···O/N are within 1.46–1.86 Å and 163–177°. In the case of the two weak HBs, the distances of CH···N are more than 2.5 Å and the values of its' angle are less than 150°. The CH···O

Table 7 Bond length (*d*), angle (θ), density (ρ_c), Laplacian of electron density ($\nabla^2\rho_c$), local kinetic energy density (*G*(*r*)), local electron potential energy density (*V*(*r*)), HB energy (E_{HB}), and second order perturbation energy ($E^{(2)}$) for complexes including 8OXOA calculated at B3LYP/6-31G(*d*) level

Pair	H-bond	*d* (Å)	θ (°)	ρ_c (a.u.)	$\nabla^2\rho_c$ (a.u.)	*G*(*r*) (a.u.)	*V*(*r*) (a.u.)	E_{HB} (kcal/mol)	$E^{(2)}$ (kcal/mol)
Anti									
8OXOA:A	N10–H···N1	2.097	173.3	0.023	0.062	0.016	−0.016	−4.91	10.96
	C2–H···N1	2.431	149.9	0.013	0.036	0.008	−0.007	−2.26	3.76
8OXOA:C	N8–H···N1	2.073	173.5	0.024	0.065	0.017	−0.017	−5.31	19.81
	C2–H···N3	2.426	144.6	0.013	0.038	0.008	−0.007	−2.25	6.21
8OXOA:G	N10–H···O11	1.829	171.5	0.035	0.106	0.028	−0.030	−9.49	35.74
	N1–H···N1	1.938	177.1	0.033	0.085	0.024	−0.026	−8.29	32.10
8OXOA:U	N10–H···O8	1.898	178.7	0.030	0.090	0.023	−0.024	−7.55	17.35
	N3–H···N1	1.852	177.7	0.039	0.102	0.030	−0.034	−10.66	26.12
	C2–H···O7	2.858	131.8	0.004	0.016	0.003	−0.002	−0.63	0.44
Syn									
s8OXOA:A	N10–H···N10	2.210	155.9	0.019	0.051	0.012	−0.012	−3.73	11.10
	N7–H···N1	1.856	171.9	0.039	0.100	0.029	−0.034	−10.53	47.55
	C2–H···O8	2.732	140.4	0.006	0.020	0.004	−0.003	−0.87	2.29
s8OXOA:C	N10–H···N3	2.222	158.0	0.018	0.051	0.012	−0.011	−3.56	17.64
	N7–H···O7	1.768	168.1	0.039	0.124	0.034	−0.036	−11.32	30.50
	O2′–H···O8	1.792	166.6	0.036	0.115	0.031	−0.032	−10.16	30.91
s8OXOA:G	N10–H···O11	2.821	150.3	0.003	0.016	0.003	−0.002	−0.53	0.86
	N7–H···O11	1.711	176.1	0.046	0.141	0.041	−0.046	−14.41	51.02
	N1–H···O8	1.844	169.8	0.035	0.103	0.028	−0.030	−9.50	28.05
	N10–H···O8	2.536	136.1	0.007	0.029	0.006	−0.004	−1.21	1.70
s8OXOA:U	N7–H···O8	1.750	172.4	0.041	0.131	0.036	−0.039	−12.32	43.65
	N3–H···O8	1.866	176.6	0.032	0.095	0.025	−0.026	−8.31	22.46

distances are near to 3.0 Å while the angles are smaller than 140°. These parameters are consistent with the investigation [10] based on nucleobases pairs, implying that the properties of intermolecular HBs retain the same in the form of nucleobase and nucleotide. Furthermore, a good linear correlation for electron density and HB distance [10] confirm the fact that the idea geometries of HB contribute to the sufficient overlap between donor and accepter orbital, strengthening the H-bonding interaction.

As it can be seen from energetic and HB analysis, s8OXOA:G complex is considered as the most stable complex due to the four intermolecular HBs based on the indication that the number of HB corresponds to stability of complex [70]. However, many complexes are not in consistent with the indication. For example, both s8OXOA:A and s8OXOA:C comprise 3 HBs, but s8OXOA:C exhibits more stable than s8OXOA:A (s8OXOA:C: −13.80 kcal/mol, s8OXOA:A: −8.95 kcal/mol). It can be explained that a CH···O in s8OXOA:A complex weakens the stability of s8OXOA:A complex. Although s8OXOA:U has only two HBs, one less than that of s8OXOA:C, its stability is stronger than that of s8OXOA:C. It can be interpreted that HBs in s8OXOA:U present a more optimal geometry, increasing interactions of HBs which make the complex more stable. Therefore, the conformer's stability is not directly related to the number of HBs, it significantly depends on the species and geometry which determine the HB property.

As it mentioned above, NH···O is served as a strong HB in most complexes according to the AIM and NBO analysis. However, it is noted that the two abnormal NH···Os (N10–H···O11, N10–H···O8) occur in s8OXOA:G in the form of weak HBs, which are similar to CH···O. It is observed that the O54 and O35, respectively take part in two intermolecular NH···Os. Because of the space configuration of s8OXOA:G, it is impossible to satisfy each HB in optimal geometry at the same time, thus one of the HBs has to exist in the form of a weak HB.

As for s8OHA:C complex, it has two intermolecular HBs namely N7–H···N8 and N3–H···O8. Geometrical analysis shows that hydrogen migration takes place in both HBs. In the case of N7–H···N8, H atom transferred from amino-group in C to N7 of s8OHA after optimization. For N3–H···O8, H which belonged to hydroxyl group previously forms covalent bond with N3 in C leading to a new electronic donor and acceptor. It is indicated that hydrogen

Table 8 Bond length (d), angle (θ), density (ρ_c), Laplacian of electron density ($\nabla^2\rho_c$), local kinetic energy density ($G(r)$), local electron potential energy density ($V(r)$), HB energy (E_{HB}), and second order perturbation energy ($E^{(2)}$) for complexes including 2OHA calculated at B3LYP/6-31G(d) level

Pair	H-bond	d (Å)	θ (°)	ρ_c (a.u.)	$\nabla^2\rho_c$ (a.u.)	$G(r)$ (a.u.)	$V(r)$ (a.u.)	E_{HB} (kcal/mol)	$E^{(2)}$ (kcal/mol)
Anti									
2OHA:A	N10–H···N1	1.988	169.4	0.029	0.078	0.021	−0.022	−7.04	32.11
	O2–H···N1	1.803	167.8	0.043	0.109	0.033	−0.039	−12.19	73.64
2OHA:C	N8–H···N1	1.939	172.5	0.032	0.086	0.024	−0.026	−8.14	37.94
	O2–H···N3	1.832	169.9	0.039	0.103	0.030	−0.035	−10.86	69.96
2OHA:G	N10–H···O11	1.893	179.7	0.031	0.091	0.024	−0.025	−7.78	30.33
	N1–H···N1	1.906	173.4	0.035	0.090	0.026	−0.029	−9.23	28.69
	O2–H···N10	2.041	151.7	0.026	0.071	0.018	−0.019	−5.95	0.11
2OHA:U	N10–H···O8	1.922	177.4	0.029	0.086	0.022	−0.022	−7.04	24.97
	N3–H···N1	1.850	177.0	0.040	0.099	0.030	−0.035	−10.89	57.45
	O2–H···O7	1.840	167.5	0.033	0.102	0.027	−0.028	−8.78	36.96
Syn									
s2OHA:A	N10–H···N7	2.046	171.0	0.025	0.069	0.017	−0.018	−5.56	11.83
	C8–H···N1	2.367	142.0	0.015	0.042	0.009	−0.009	−2.69	4.37
s2OHA:C	N8–H···N7	2.092	169.8	0.022	0.061	0.015	−0.015	−4.76	15.69
	C8–H···N3	2.200	143.0	0.020	0.059	0.014	−0.013	−4.17	11.83
	C2′–H···O7	2.705	175.1	0.006	0.021	0.004	−0.003	−0.90	1.04
s2OHA:G	N10–H···O11	1.859	166.8	0.032	0.100	0.026	−0.027	−8.43	31.09
	N1–H···N7	1.906	173.6	0.034	0.092	0.026	−0.029	−8.95	34.9
s2OHA:U	N10–H···O8	1.913	167.8	0.028	0.087	0.022	−0.022	−6.98	15.77
	N3–H···N7	1.822	176.4	0.041	0.109	0.032	−0.036	−11.45	27.96
	C8–H···O7	2.832	120.8	0.004	0.018	0.003	−0.002	−0.70	0.41

migration is in favor of stability of complex. As it can be seen in Table 6, the intermolecular HBs of s8OHA:A tend to transfer H atom from one nucleobases to the other. As a new HB O8–H···N1 after optimization, the distance is 1.46 Å and the angle is 173.9°. According to AIM analysis, the values of ρ_c and$\nabla^2\rho_c$ of this HB (0.085, 0.189 a.u.) exceed the upper limit of the criteria for HB, these results are in good agreement with NBO analysis that $E^{(2)}$ is 87.02 kcal/mol which is larger than other NH···Os. This confirms the necessary of this hydrogen transference. The phenomenon of hydrogen migration can be illustrated that interaction of two monomers causes the H atom to prefer the atom with more negative charge.

In general, the interaction between two nucleotides is only concentrated on their base pairs. An interesting phenomenon shows that an OH in furanose ring of C participates in OH···O with O atom in C=O in 8 position of s8OXOA in s8OXOA:C complex. Furthermore, it is demonstrated that this HB has high values of ρ_c and $\nabla^2\rho_c$ (0.036, 0.115 a.u.) which agrees well with the $E^{(2)}$ up to 30.91 kcal/mol. All the parameters suggest that this HB improves the complex's stability. However, taking this complex into the whole DNA and RNA spiral structure, it means that this configuration results in the chain's distortion which significantly influences next biological process such as translation of genetic code.

Intramolecular HB analysis of oxidative 2′-deoxyadenosine nucleotides

The intramolecular HBs of all the oxidative 2′-deoxyadenosine nucleotides investigated are presented in supplementary material, showing that there is only slight difference of intramolecular HBs compared with the form of complex and monomer.

In the case of anti/syn 2OHA, it is obvious that anti 2OHA is stabilized mainly by the OH···O between OH in phosphate group and O atom in furanose ring based on AIM and NBO analysis. With the rotation of glucosidic bond this OH prefers to combine with N atom in base leading to a stronger interaction. It is observed that 8OHA has a CH···O between furanose ring and base and is considered as a weak HB according to the criteria of AIM analysis. However, for this CH···O, the hyperconjugation between O atom lone pair orbital and X–H σ^* antibonding orbital only occurs in complexes indicating that the CH···O in monomer belongs to electrostatic interaction and the formation of complex helps the CH···O become a real

Table 9 Bond length (d), angle (θ), density (ρ_c), Laplacian of electron density ($\nabla^2\rho_c$), local kinetic energy density ($G(r)$), local electron potential energy density ($V(r)$), HB energy (E_{HB}), and second order perturbation energy ($E^{(2)}$) for complexes including fapyA calculated at B3LYP/6-31G(d) level

Pair	H-bond	d (Å)	θ (°)	ρ_c (a.u.)	$\nabla^2\rho_c$ (a.u.)	$G(r)$ (a.u.)	$V(r)$ (a.u.)	E_{HB} (a.u.)	$E^{(2)}$ (kcal/mol)
Anti									
fapyA:A	N10–H···N1	2.042	174.4	0.026	0.069	0.018	−0.019	−5.83	13.37
	C2–H···N1	2.498	146.9	0.012	0.032	0.007	−0.006	−1.91	3.04
fapyA:C	N8–H···N1	2.011	175.3	0.028	0.073	0.019	−0.021	−6.43	15.12
	C2–H···N3	2.473	143.3	0.012	0.035	0.008	−0.006	−2.00	2.84
fapyA:G	N10–H···O11	1.920	177.7	0.029	0.086	0.022	−0.023	−7.08	15.93
	N1–H···N1	1.920	177.9	0.034	0.088	0.025	−0.028	−8.77	21.67
fapyA:U	N10–H···O8	1.994	179.6	0.024	0.073	0.018	−0.018	−5.61	12.6
	N3–H···N1	1.829	178.3	0.041	0.105	0.031	−0.037	−11.47	28.23
	C2–H···O7	2.792	132.6	0.005	0.019	0.004	−0.002	−0.76	0.57
Syn									
sfapyA:A	N10–H···O8	1.947	171.8	0.027	0.081	0.021	−0.021	−6.62	20.15
	C8–H···N1	2.363	141.8	0.015	0.042	0.010	−0.009	−2.81	8.34
sfapyA:C	N8–H···O8	1.940	170.3	0.028	0.081	0.021	−0.021	−6.74	21.59
	C8–H···N3	2.271	137.9	0.018	0.052	0.012	−0.011	−3.53	8.48
sfapyA:G	N10–H···O8	2.075	150.8	0.019	0.065	0.015	−0.013	−4.23	6.88
	N1–H···O8	2.211	142.1	0.014	0.052	0.011	−0.009	−2.84	4.22
	N1–H···N10	2.661	133.8	0.007	0.030	0.006	−0.004	−1.24	0.84
	N10–H···O11	2.026	143.5	0.023	0.073	0.017	−0.017	−5.24	9.71
sfapyA:U	N10–H···O8	2.113	135.6	0.018	0.062	0.014	−0.012	−3.91	8.23
	N3–H···O8	1.859	161.5	0.031	0.101	0.026	−0.026	−8.18	26.68

HBs. With regard to syn 8OHA, a CH···N interaction in syn 8OHA only exists in s8OHA:A based on AIM analysis, but the NBO analysis shows that there is no hyperconjugation relevant to the N lone pair orbital and C–H σ^* antibonding orbital. Therefore, this CH···N is classified as electrostatic interaction. In the case of anti/syn 8OXOA, an OH of phosphate group served as proton donor combines with O or N in base to form OH···O/N HB. It is obvious that the angle of the HB between phosphate group and base is more linear than that of HB between phosphate group and sugar fragment. Thus it is no doubt that the electronic donor in base is the first choice to OH in phosphate group. As for anti/syn fapyA, an intramolecular NH···O HB is formed in base. On the basis of geometrical, AIM and NBO analysis, this HB is not influenced by the conformer of anti/syn fapyA, and it has stronger interaction in sfapyA:A and sfapyA:C complexes. Furthermore, in anti fapyA, an O atom in phosphate group is employed as electronic donor to combine with two NH in base at the same time. Although a CH···O satisfy the criteria for HB based on AIM analysis, there is no donor–acceptor orbital interaction found in this CH···O, thus this CH···O only belongs to electrostatic interaction. In the case of syn fapyA, C2–H···O1 is considered as a weak HB except in sfapyA:G complex. For C2′–H···N3, it is treated as a weak HB in monomers and most complex, however, the BCP of this CH···N is not found in sfapyA:G complex indicating that there is no interaction between N and CH.

In addition, as for intramolecular HB involving oxidative 2′-deoxyadenosine nucleotides and RNA nucleotides, the relationship between $G(r)$ and E_{HB}, as well as $G(r)$ and HB distance was also investigated. The results are presented in support material, showing that $G(r)$ is related exponentially with HB distance, and has linear fitting with E_{HB}. These results are in good agreement with that ones with respect to intermolecular HBs. Furthermore, comparing E_{HB} to $E^{(2)}$, they are also consistent with each other to estimate the strength of intramolecular HBs. In some cases, the values of E_{HB} about -1.00 kcal/mol correspond to the absent values of $E^{(2)}$. This situation is similar with the one reported before [71], suggesting that it is related to the HB enthalpy due to the repulsive interaction in HB.

Intramolecular HB analysis of RNA nucleotides

The geometry and properties of intramolecular HBs of RNA nucleotides are listed in supplementary material. It is clear that these HBs almost remain the same in the form of monomer and complex. In the case of A, an OH···O formed by O atom in phosphate group and OH in furanose ring has the strongest interaction due to its high values of

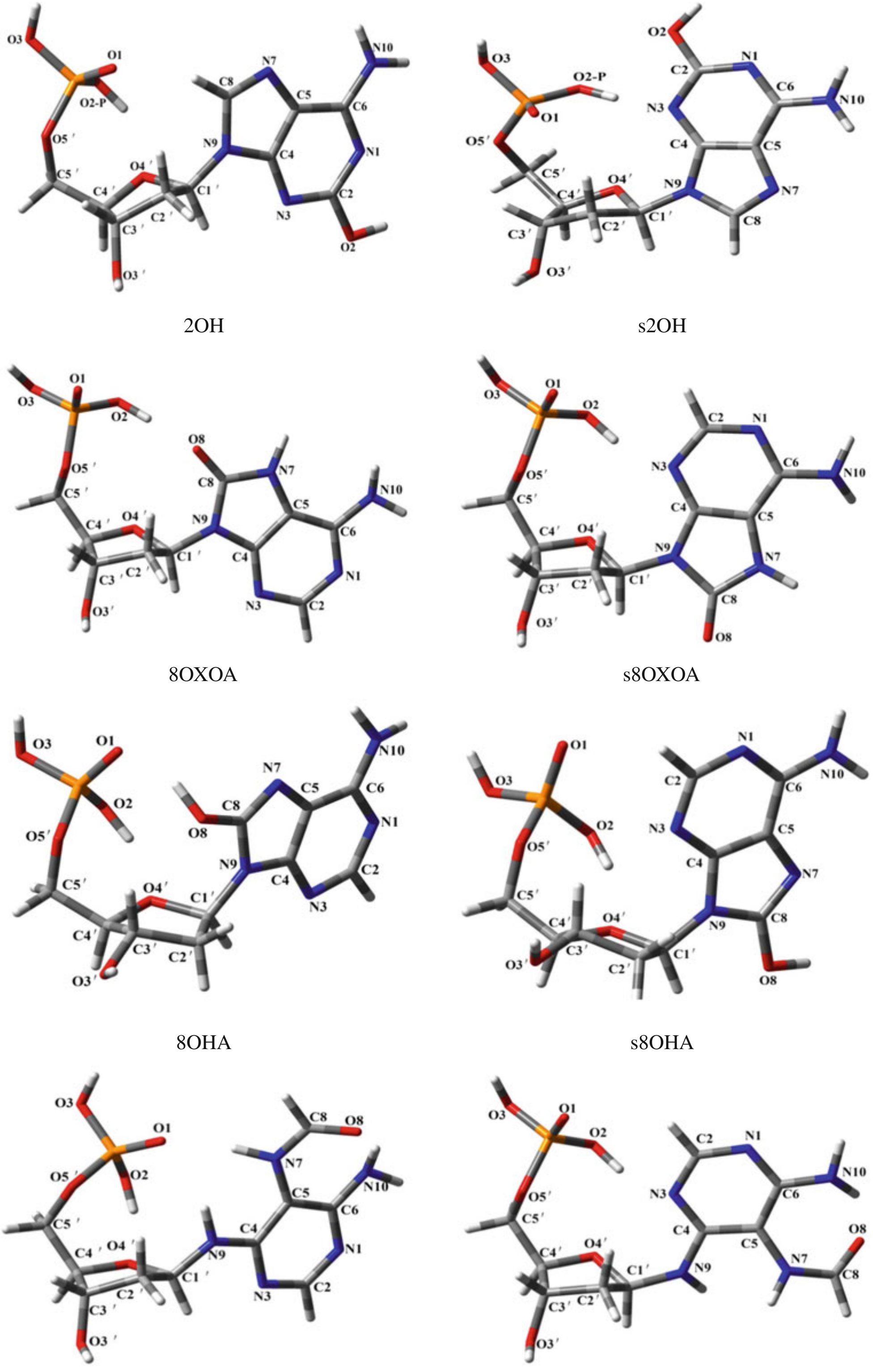

2OH s2OH

8OXOA s8OXOA

8OHA s8OHA

fapyA sfapyA

Fig. 1 Optimized structures of oxidative 2′-deoxyadenosine nucleotides

parameters. Another HB, CH···O between base and phosphate group, it meets the criteria for HB based on AIM and NBO analysis, thus it is considered as a true HB. As for C, it is shown that the two CH···Os in C exist BCP which is served as the requirement and first criteria for determining any chemical bond, but there is no hyperconjugative

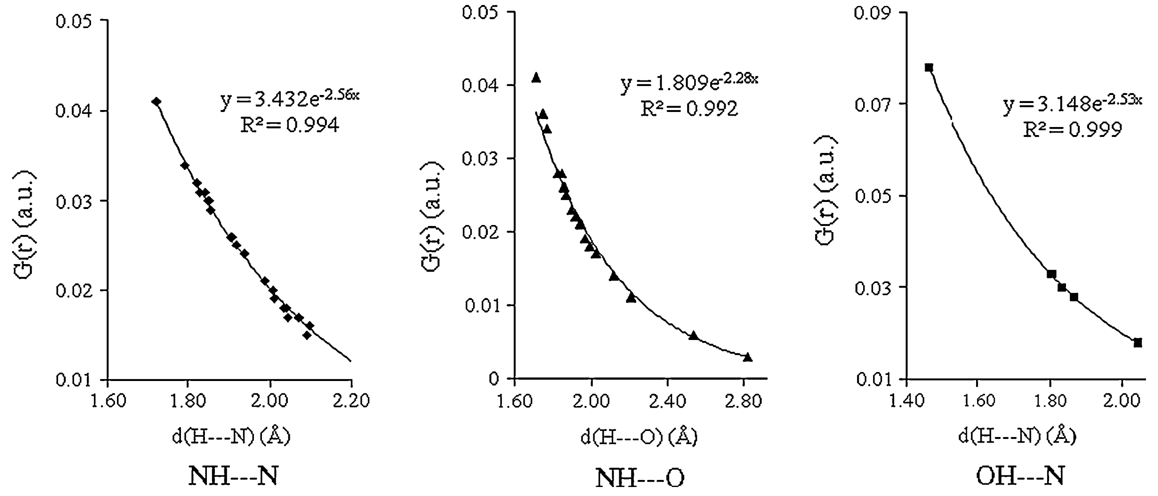

Fig. 2 The exponential relationship between local kinetic energy density $G(r)$ and HB distance of intermolecular NH···N, NH···O and OH···N

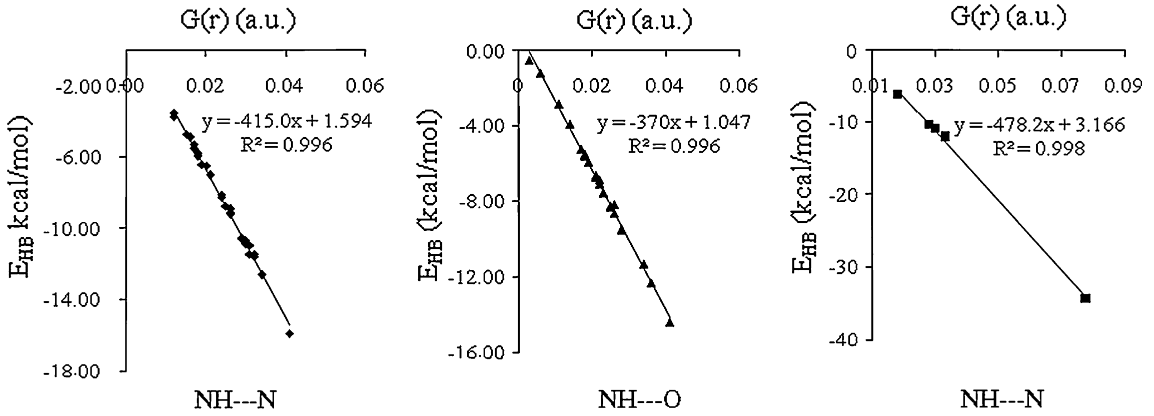

Fig. 3 The linear relationship between local kinetic energy density $G(r)$ and HB energy (E_{HB}) of intermolecular NH···N, NH···O, OH···N

interaction from the lone pair of O to an antibonding σ^* orbital of C–H. As a result, the two CH···Os should be considered as electrostatic interaction. This situation can be illustrated that the presence of BCP reflects the existence of interaction between two atoms. However, to classify its interaction, a more detail investigation is necessary. In addition, because an OH in furanose in C participates in intermolecular HB in s8OXOA:C complex, this OH cannot take part in intramolecular HB with base in s8OXOA:C complex. Therefore, there is not any BCP and interaction found between the two atoms. It is shown that G is stabilized mainly by the intramolecular HB between phosphate group and furanose. Meanwhile, the two CH···Os are classified as true HBs because they not only meet the criteria for HB but also exist hyperconjugative interaction. In addition, it is also found that an OH···O HB of which both electronic donor and acceptor are in sugar fragment has similar property with CH···O HB between phosphate group and base. However, this OH···O is impossible in RNA because this O atom of the OH is involved in a phosphodiester linkage with a neighboring nucleotide. Therefore this OH···O is only observed in isolated nucleotide. In the case of U, O2′ is, respectively acted as electronic donor and acceptor to form two intramolecular OH···O HBs which make contribution to the stability. It should be noted that the OH···O formed in furanose ring as well as that mentioned in G, only occurs in isolated nucleotide.

Conclusion

In this article, the interactions between oxidative 2′-deoxyguanosine nucleotides and RNA nucleotides were investigated at B3LYP/6-31G(d) level. It is revealed that the syn 8OXOA:G complex is the most stable among all the complexes discussed here. It is also obvious that the species and position of substitution of 2′-deoxyadenosine nucleotide have a significant effect on the stability of complex. In addition, these interactions are significantly relevant to types and geometry of intermolecular HB. According to AIM and NBO analysis, the intermolecular NH···N/O and OH···O/N HBs are crucial to stability of complexes. The intermolecular CH···N/O, especially CH···O which has faint hyperconjugative interaction is classified as weak HBs taking the criteria for HB into account. In order to form more stable complex the hydrogen migration occurs in s8OHA:C complex as well as the phenomenon that an OH of furanose ring participate in intermolecular HB in s8OXOA:C complex.

The intramolecular HBs of all the monomers and complexes are also studied. It is suggested that the OH···O/N and CH···O/N exist in oxidative 2′-deoxyguanosines nucleotide while OH···O and CH···O exist in RNA nucleotide. In some cases CH···O is only considered as electrostatic interaction due to its absence of hyperconjugative interaction. It is worth noting that there is only slight difference of intramolecular HB between monomers and complexes.

Acknowledgments Financial supports from National Natural Science Foundation of China (20875038) and the Research Program of State Key Laboratory of Food Science and Technology (SKLF -TS-200907) are acknowledged.

References

1. Kolandaivel P, Deepa P (2008) Studies on tautomeric forms of Guanine–Cytosine base pairs of nucleic acids and their interactions with water molecules. J Biomol Struct Dyn 25:733–746
2. Zhang RQ, Fan WJ, Liu SB (2007) Computation of large systems with an economic basis set: structures and reactivity indices of nucleic acid base pairs from density functional theory. J Comput Chem 28:967–974
3. Shishkin OV, Gorb L, Zhikol OA, Leszczynski J (2004) Conformational analysis of c anonical 2-deoxyribonucleotides. 1. Pyrimidine nucleotides. J Biomol Struct Dyn 21:537–553
4. Shishkin OV, Palamarchuk GV, Gorb L, Leszczynski J (2009) Dependence of deformability of geometries and characteristics of intramolecular hydrogen bonds in canonical 2′-deoxyribonucleotides on DNA conformations. J Biomol Struct Dyn 26:653–661
5. Hovorun DM, Yurenko YP, Zhurakivsky RO, Samijlenko SP (2011) Intramolecular CH–O hydrogen bonds in the AI and BI DNA-like conformers of canonical nucleosides and their Watson–Crick pairs. Quantum chemical and AIM analysis. J Biomol Struct Dyn 29:51–65
6. Yakushevich LV (2011) DNA structure and dynamics: potential of interactions between two complementary DNA bases. Int J Quantum Chem 111:2482–2489
7. Gorb L, Shishkin O, Leszczynski J (2005) Charges of phosphate groups. A role in stabilization of 2′-deoxyribonucleotides. A DFT investigation. J Biomol Struct Dyn 22:441
8. Shishkin OV, Gorb L, Zhikol OA, Leszczynski J (2004) Conformational analysis of canonical 2-deoxyribonucleotides. 1. Pyrimidine nucleotides. J Biomol Struct Dyn 21:537–553
9. Shishkin OV, Gorb L, Zhikol OA, Leszczynski J (2004) Conformational analysis of canonical 2-deoxyribonucleotides. 2. Purine nucleotides. J Biomol Struct Dyn 22:227–243
10. Mohajeri A, Nobandegani FF (2008) Detection and evaluation of hydrogen bond strength in nucleic acid base pairs. J Phys Chem A 112:281–295
11. Zimmerman SC, Quinn JR, Del Bene JE, Shavitt I (2007) Does the A–T or G–C base-pair possess enhanced stability? Quantifying the effects of CH–O interactions and secondary interactions on base-pair stability using a phenomenological analysis and ab initio calculations. J Am Chem Soc 129:934–941
12. Sponer JE, Leszczynski J, Sychrovsky V, Sponer J (2005) Sugar edge/sugar edge base pairs in RNA: stabilities and structures from quantum chemical calculations. J Phys Chem B 109:18680–18689
13. Brandl M, Meyer M, Suhnel J (2001) Quantum-chemical analysis of C–H–O and C–H–N interactions in RNA base pairs—H-bond versus anti-H-bond pattern. J Biomol Struct Dyn 18:545–555
14. Bhattacharyya D, Roy A, Panigrahi S, Bhattacharyya M (2008) Structure, stability, and dynamics of canonical and noncanonical base pairs: quantum chemical studies. J Phys Chem B 112:3786–3796
15. Lamsabhi M, Alcami M, Mo O, Bouab W, Esseffar M, Abboud JLM, Yanez M (2000) Are the thiouracils sulfur bases in the gas-phase? J Phys Chem A 104:5122–5130
16. Qiu ZM, Wang HJ, Xia YM (2010) The effect of oxidation on the stability of G:C base pair: a MP2 study. Struct Chem 21:931–937
17. LA Popelier P, Xue CX (2009) Prediction of interaction energies of substituted hydrogen-bonded Watson–Crick cytosine: guanine (8X) base pairs. J Phys Chem B 113:3245–3250
18. Meng FC, Wang HJ, Xu WR, Liu CB (2005) Theoretical study of GC^+/GC base pair derivatives. Chem Phys 308:117–123
19. Guerra CF, Bickelhaupt FM, Snijders JG, Baerends EJ (1999) The nature of the hydrogen bond in DNA base pairs: the role of charge transfer and resonance assistance. Chem Eur J 5:3581–3594
20. Hocquet A, Leulliot N, Ghomi M (2000) The peculiar role of cytosine in nucleoside conformational behaviour: hydrogen bond donor capacity of nucleic bases. J Phys Chem B 104:4560–4568
21. Foloppe N, Hartmann B, Nilsson L, MacKerell AD Jr (2002) Intrinsic conformational energetics associated with the glycosyl torsion in DNA: a quantum mechanical study. Biophys J 82:1554–1569
22. Shim JE, Przybylski JL, Wetmore SD (2010) Effects of nucleophile, oxidative damage, and nucleobase orientation on the glycosidic bond cleavage in deoxyguanosine. J Phys Chem B 14: 2319–2326
23. Millen AL, Wetmore SD, Manderville RA (2010) Conformational flexibility of C8-phenoxyl-2′-deoxyguanosine nucleotide adducts. J Phys Chem B 114:4373–4382
24. Cysewski P (1999) Structure and properties of hydroxyl radical modified nucleic acid components:pairing properties of 2-hydroxyadenine and 8-oxoadenine. J Mol Struct (Theochem) 466: 59–67
25. Graziewicz MA, Zastawny TH, Olinski R, Speina E, Siedlecki J, Tudek B (2000) Fapyadenine is a moderately efficient chain terminator for prokaryotic DNA polymerases. Free Radical Biol Med 28:75–83
26. Hashiguchi K, Zhang QM, Sugiyama H, Ikeda S, Yonei S (2002) Characterization of 2-hydroxyadenine DNA glycosylase activity of *Escherichia coli* MutY protein. Int J Radiat Biol 78:585–592
27. Whiteman M, Hong HS, Jenner A, Halliwell B (2002) Loss of oxidized and chlorinated bases in DNA treated with reactive oxygen species: implications for assessment of oxidative damage in vivo. Biochem Biophys Res Commun 296:883–889
28. Haran′czyk M, Miller JH, Gutowski M (2007) Differences in electrostatic potential around DNA fragments containing adenine and 8-oxo-adenine. An analysis based on regular cylindrical projection. J Mol Graph Model 26:282–289
29. Lee C, Yang W, Parr RG (1988) Development of the Colle-Salvetti correlation-energy formula into a functional of the electron density. Phys Rev B 37:785–789

30. Becke AD (1993) Density-functional thermochemistry. III. The role of exact exchange. J Chem Phys 98:5648–5652
31. Becke AD (1988) Density-functional exchange-energy approximation with correct asymptotic behavior. Phys Rev A 38:3098–3100
32. Hovorun DM, Yurenko YP, Zhurakivsky RO, Samijlenko SP, Ghomi M (2007) The whole of intramolecular H-bonding in the isolated DNA nucleoside thymidine. AIM electron density topological study. Chem Phys Lett 447:140–146
33. Millen AL, Churchill CDM, Manderville RA, Wetmore SD (2010) Effect of Watson–Crick and Hoogsteen base pairing on the conformational stability of c8-phenoxyl-2′-deoxyguanosine adducts. J Phys Chem B 114:12995–13004
34. Qiu WY, Zhou PP (2009) Red-shifted hydrogen bonds and blue-shifted van der Waals contact in the standard Watson–Crick adenine-thymine base pair. J Phys Chem A 113:10306–10320
35. Sponer J, Jurecka P, Hobza P (2004) Accurate interaction energies of hydrogen-bonded nucleic acid base pairs. J Am Chem Soc 126:10142–10151
36. Hobza P, Zahradnik R (1988) Intermolecular complexes. Elsevier, Amsterdam
37. Boys SB, Bernardi F (1970) The calculation of small molecular interactions by the differences of separate total energies. Some procedures with reduced errors. Theor Chim Acta 19:533–566
38. Simon S, Duran M, Dannenberg JJ (1996) How does basis set superposition error change their potential-energy surfaces? J Chem Phys 105:11024–11031
39. Frisch MJ, Trucks GW, Schlegel HB, Scuseria GE, Robb MA, Cheeseman JR, Montgomery JA, Vreven T Jr, Kudin KN, Burant JC, Millam JM, Iyengar SS, Tomasi J, Barone V, Mennucci B, Cossi M, Scalmani G, Rega N, Petersson GA, Nakatsuji H, Hada M, Ehara M, Toyota K, Fukuda R, Hasegawa J, Ishida M, Nakajima T, Honda Y, Kitao O, Nakai H, Klene M, Li X, Knox JE, Hratchian HP, Cross JB, Adamo C, Jaramillo J, Gomperts R, Stratmann RE, Yazyev O, Austin AJ, Cammi R, Pomelli C, Ochterski JW, Ayala PY, Morokuma K, Voth GA, Salvador P, Dannenberg JJ, Zakrzewski VG, Dapprich S, Daniels AD, Strain MC, Farkas O, Malick DK, Rabuck AD, Raghavachari K, Foresman JB, Ortiz JV, Cui Q, Baboul AG, Clifford S, Cioslowski J, Stefanov BB, Liu G, Liashenko A, Piskorz P, Komaromi I, Martin RL, Fox DJ, Keith T, Al-Laham MA, Peng CY, Nanayakkara A, Challacombe M, Gill PMW, Johnson B, Chen W, Wong MW, Gonzalez C, Pople JA (2003) Gaussian03. Gaussian Inc, Wallingford
40. Bader RFW (1990) Atoms in molecules: a quantum theory. Clarendon Press, Oxford
41. Reed AE, Weinstock RB, Weinhold F (1985) Natural population analysis. J Chem Phys 83:735–746
42. Popelier PLA (1998) Characterization of a dihydrogen bond on the basis of the electron density. J Phys Chem A 102:1873–1878
43. Koch U, Popelier PLA (1995) Characterization of C–H–O hydrogen bonds on the basis of the charge density. J Phys Chem 99:9747–9754
44. Espinosa E, Lecomte C, Molins E (1998) Hydrogen bond strengths revealed by topological analyses of experimentally observed electron densities. Chem Phys Lett 285:170–173
45. Abramov YA (1997) On the possibility of kinetic energy density evaluation from the experimental electron-density distribution. Acta Crystallogr A 53:264–272
46. Espinosa E, Molins E, Lecomte C (1999) Experimental electron density overlapping in hydrogen bonds: topology vs. energetics. Chem Phys Lett 285:170–173
47. Carpenter JE, Weinhold F (1988) Analysis of the geometry of the hydroxymethyl radical by the different hybrids for different spins natural bond orbital procedure. J Mol Struct (Theochem) 169: 41–62
48. Foster JP, Weinhold F (1980) Natural hybrid orbitals. J Am Chem Soc 102:7211–7218
49. Reed AE, Weinhold F (1983) Natural bond orbital analysis of near-Hartree-Fock water dimer. J Chem Phys 78:4066–4073
50. Wiberg KB (2004) Basis set effects on calculated geometries: 6-311++G** vs. aug-cc-pVDZ. J Comput Chem 25:1342–1346
51. Grabarkiewicz T, Hoffmann M (2006) Syn- and anti-conformations of 5′-deoxy- and 5′-*O*-methyl-uridine 2′,3′-cyclic monophosphate. J Mol Model 12:205–212
52. Cheng X, Kelso C, Hornak V, de los Santos C, Grollman AP, Simmerling C (2005) Dynamic behavior of DNA base pairs containing 8-oxoguanine. J Am Chem Soc 127:13906–13918
53. Kamiya H, Miura H, Murata-Kamiya N, Ishikawa H, Sakaguchi T, Inoue H, Sasaki T, Masutani C, Hanaoka F, Nishimura S, Ohtsuka E (1995) 8-Hydroxyadenine (7,8-dihydro-8-oxoadenine) induces misincorporation in in vitro DNA synthesis and mutations in NIH3T3 cells. Nucleic Acids Res 23:2893–2899
54. Taniguchi Y, Kool ET (2007) Nonpolar isosteres of damaged DNA bases: effective mimicry of mutagenic properties of 8-oxopurines. J Am Chem Soc 129:8836–8844
55. Lipscomb L, Peek M, Morningstar M, Verghis S, Miller E, Rich A, Essigmann J, Williams L (1995) X-ray structure of a DNA decamer containing 7,8-dihydro-8-oxoguanine. Proc Natl Acad Sci USA 92:719–723
56. McAuley-Hecht KE, Leonard GA, Gibson NJ, Thomson JB, Watson WP, Hunter WN, Brown T (1994) Crystal-structure of a DNA duplex containing 8-hydroxydeoxyguanine-adenine base-pairs. Biochemistry 33:10266–10270
57. Hamm ML, Parker AJ, Steele TWE, Carman JL, Parish CA (2010) Oligonucleotide incorporation and base pair stability of 9-deaza-2′-deoxyguanosine, an analogue of 8-oxo-2′-deoxyguanosine. J Org Chem 75:5661–5669
58. Sintim HO, Kool ET (2006) Remarkable sensitivity to DNA base shape in the DNA polymerase active site. Angew Chem Int Ed 45:1974–1979
59. Kincaid KK, Beckman J, Zivkovic A, Halcomb RL, Engels JW, Kuchta RD (2005) Exploration of factors driving incorporation of unnatural dNTPS in DNA by Klenow fragment (DNA polymerase I) and DNA polymerase alpha. Nucleic Acids Res 33:2620–2628
60. Zhang X, Lee I, Berdis AJ (2005) Rational attempts to optimize non-natural nucleotides for selective incorporation opposite an abasic site. Biochemistry 45:3293–13303
61. Fonseca Guerra C, van der Wijst T, Bickelhaupt FM (2006) Nanoswitches based on DNA base pairs: why adenine-thymine is less suitable than guanine-cytosine. Chem Phys Chem 7:1971–1979
62. Szatylowicz H, Sadlej-Sosnowska N (2010) Characterizing the strength of individual hydrogen bonds in DNA base pairs. J Chem Inf Model 50:2151–2161
63. Grunenberg J, Streubel R, Frantzius GV (2003) The strongest bond in the universe? Accurate calculation of compliance matrices for the ions NH, HCO, and HOC. J Chem Phys 119: 165–169
64. Shiskhin OV, Hobza P, Sponer J (1999) Intramolecular flexibility of DNA bases in adenine-thymine and guanine-cytosine Watson–Crick base pairs. J Mol Struct 477:15–21
65. Grabowski SJ, Sokalski WA, Leszczynski J (2006) The possible covalent nature of N–H…O hydrogen bonds in formamide dimer and related systems: an ab initio study. J Phys Chem A 110:4772–4779
66. Lo Presti L, Soave R, Destro R (2006) On the interplay between CH…O and OH…O interactions in determining crystal packing and molecular conformation: an experimental and theoretical charge density study of the fungal secondary metabolite austdiol (C12H12O5). J Phys Chem B 110:6405–6414

67. Galvez O, Gomez P, Pacios L (2001) Approximate kinetic energy density for intermolecular regions in hydrogen bond dimers. Chem Phys Lett 337:263–268
68. Wojtulewski S, Grabowski SJ (2003) DFT and AIM studies on two-ring resonance assisted hydrogen bonds. J Mol Struct (Theochem) 621:285–291
69. Rozas I (2007) On the nature of hydrogen bonds: an overview on computational studies and a word about patterns. Phys Chem Chem Phys 9:2782–2790
70. Battersby T, Benner S (2003) Nucleobase pairing in Watson–Crick-like genetic expanded information systems. Structure 11: 1485–1498
71. Deshmukh MM, Gadre SR, Bartolotti LJ (2006) Estimation of intramolecular hydrogen bond energy via molecular tailoring approach. J Phys Chem A 110:12519–12523